

Video Article

Laminectomy and Spinal Cord Window Implantation in the Mouse

Elizabeth A. Pietruczyk¹, Terilyn K.L. Stephen², Simon Alford¹, Sarah E. Lutz¹

¹Department of Anatomy and Cell Biology, University of Illinois at Chicago College of Medicine

²Medical Scientist Training Program, University of Illinois at Chicago College of Medicine

Correspondence to: Sarah E. Lutz at selutz@uic.edu

URL: <https://www.jove.com/video/58330>

DOI: [doi:10.3791/58330](https://doi.org/10.3791/58330)

Keywords: Spinal cord, laminectomy, mouse, two-photon, cranial window, blood-brain barrier

Date Published: 8/9/2018

Citation: Pietruczyk, E.A., Stephen, T.K., Alford, S., Lutz, S.E. Laminectomy and Spinal Cord Window Implantation in the Mouse. *J. Vis. Exp.* (), e58330, doi:10.3791/58330 (2018).

Abstract

This protocol describes a method for spinal cord laminectomy and glass window implantation for *in vivo* imaging of the mouse spinal cord. An integrated digital vaporizer is utilized to achieve a stable plane of anesthesia at a low-flow rate of isoflurane. A single vertebral spine is removed, and a commercially available cover-glass is overlaid on a thin agarose bed. A 3D-printed plastic backplate is then affixed to the adjacent vertebral spines using tissue adhesive and dental cement. A stabilization platform is used to reduce motion artifact from respiration and heartbeat. This rapid and clamp-free method is well-suited for acute multi-photon fluorescence microscopy. Representative data are included for an application of this technique to two-photon microscopy of the spinal cord vasculature in transgenic mice expressing eGFP:Claudin-5 — a tight junction protein.

Introduction

Transgenic animal models expressing fluorescent proteins, when combined with intravital microscopy, provide a powerful platform for addressing biology and pathophysiology. To apply these techniques to the spinal cord, specialized protocols are required to prepare the spinal cord for imaging. One such strategy is to conduct a laminectomy and spinal cord window implantation. The key features of an ideal laminectomy protocol for microscopy include preservation of native tissue structure and function, stability of the imaging field, quick processing time, and reproducibility of results. A particular challenge is to stabilize the imaging field against the motion induced by respiration and heartbeat. Multiple *ex vivo* and *in vivo* strategies have been reported to achieve these goals^{1,2,3,4,5}. Most *in vivo* methods involve clamping the sides of the spinal column^{2,4} and is often followed by implanting a rigid metal apparatus^{3,4} for stability during surgery and downstream imaging applications. Clamping the spinal column can potentially compromise blood flow and induce blood-brain barrier (BBB) protein remodeling.

The purpose of this method is to make the intact spinal cord available for optical imaging in the living mouse while minimizing the invasiveness of the protocol and improving outcomes. We describe a single laminectomy and cover-glass implantation procedure paired with a minimally invasive oval plastic 3D-printed backplate that still achieves robust mechanical stability. The backplate is directly adhered to the anterior and posterior vertebral spines with dental cement. The backplate is equipped with lateral extension arms with screw holes that rigidly attach to the microscope stage via a metal arm. This effectively anchors the intact anterior and posterior vertebra to the microscope stage, providing mechanical resistance to the motion artifact that would otherwise be introduced by respiration and heartbeat. The method has been optimized for laminectomy of a single vertebra at thoracic level 12, omitting the clamps utilized in alternative strategies for stability during *in vivo* imaging. The procedure is rapid, taking approximately 30 min per mouse.

This protocol can be used to study disease mechanisms of the BBB. The BBB is a dynamic microvascular system comprised of endothelial cells, vascular smooth muscle, pericytes, and astrocyte foot processes that provide a highly selective environment for the central nervous system (CNS). Representative data depict the application of this protocol in transgenic mice engineered to express enhanced green fluorescent protein (eGFP):Claudin-5, a BBB tight junction protein. The provided backplate printing files can also be customized for alternative applications.

Protocol

All experiments follow the University of Illinois, Chicago Institutional Animal Care and Use Committee protocols.

1. Reagent Preparation

1. Prepare artificial cerebral spinal fluid (aCSF) to contain 125 mM NaCl, 5 mM KCl, 10 mM Glucose, 10 mM HEPES, 2 mM MgCl₂·6H₂O, 2 mM CaCl₂·2H₂O in ddH₂O. Sterile filter and freeze in individual-use aliquots. Warm aCSF in a water bath to 39 °C before use.
2. Warm low melting-point agarose (2%) in aCSF until fully dissolved in a water bath set to 65 °C. During the laminectomy, cool the melted agarose aliquot to 39 °C in a water bath, so that it can be ready at close to physiologic temperature for step 5.2.
Note: The agarose solution can be stored at -20 °C in single-use aliquots.
3. Prepare sterile 50 mg/mL carprofen in bacteriostatic water. Store at 4 °C.

- Clean cover-glasses with 70% ethanol, three washes of ddH₂O, and store dry in a dust-free container.

2. Backplate 3D Printing

- Use 3D CAD software is used to create a model to the dimensions shown in **Figure 1**. The interior is an ellipse widest at the bottom surface with respect to the printer and cut with a lofted cut to a smaller ellipse forming a lumen at the opposite surface. Two projecting arms with holes to accept screws extend laterally, for attachment to the backplate holding fork. From this 3D structure, create a triangulated 3D mesh file (.STL file).
Note: See **Figure 1B–D** and **Supplementary Files 1 and 2**.
- Upload the triangulated 3D mesh file to a 3D printer.
- Print backplates using a 0.4 mm hot-end nozzle and a 0.2 mm layer height. Select nozzle temperature of 205 °C, bed temperature of 45 °C, and printing speed of 45 mm/s.
- Assess the resultant 3D printed backplates visually for structural integrity (**Figure 1E**); gross structural failure (absent lumen, collapsed wall) indicates printing defects (**Figure 1F**).

3. Surgical Preparation

- Preheat the heating pad.
- Load isoflurane into the delivery syringe while working in a chemical fume hood. Attach the delivery syringe to the isoflurane unit.
- Select an 8–12-week-old mouse. Weigh the animal. Induce anesthesia using 2% isoflurane in an induction chamber. Inject carprofen at 5 mg/kg subcutaneously.
- Position the nose-cone and deliver isoflurane at 2% with a flow rate of 150 mL/min for maintenance of a surgical plane of anesthesia (**Figure 2A–E**). Wrap the heating pad with a disposable absorbent pad for ease of cleanup.
- Position an animal on the heating pad at the surgical station and install the nose cone. Lubricate the thermometer with petroleum jelly and insert it 5 mm into the rectum. Tape the thermometer probe to the tail for stability. Apply ophthalmic ointment to eyes of the mouse.
- To maintain hydration, apply 200 µL of lactated Ringer's solution by subcutaneous injection every 30 min until termination of the experiment.
- Spray the dorsum with 70% ethanol, remove fur with clippers, and clean the site with povidone-iodine.

4. Laminectomy

- Position the animal between the ear bars; these maintain the head position of the mouse with respect to the nose-cone.
- Confirm that animal is deeply anesthetized as assessed by lack of interdigital pinch reflex and steady respiratory pattern.
- Make a 1.5 cm rostral-caudal incision at midline over the lower thoracic/upper lumbar region using #11 blade (**Figure 2E**). Separate the skin by grasping it with blunt toothed forceps and/or gloved fingers. Use forceps to separate and peel back any remaining transparent connective tissue underneath the skin. The superficial musculature should now be exposed; displace this with a foam surgical spear.
- Use foam surgical spears (or a curette) to clear away the remaining, deeper musculature of the target vertebra (thoracic 12). To create a seat for the backplate, also clear away muscle from the posterior aspect of thoracic 11, and the anterior aspect of thoracic 13. Control any bleeding by applying gentle pressure with a surgical spear or use a minimal pulse with a cautery gun. Continue to remove the remaining muscle away from the tendons using forceps.
- Once muscles are removed, carefully detach the tendons by cutting with forceps. There should be plenty of space for visualizing and manipulating the cord when this step is complete. Check that the dura matter of the inter-vertebral space, the semi-transparent laminar bone, the central superficial blood vessel underneath the bone, and anterior radiating artery are now clearly visible.
- Wet the region with warm aCSF. Use the microdrill to repetitively thin the laminar bone using straight strokes parallel to the long axis of the spinal cord (**Figure 2F, Figure 3**). If desired, utilize a gliding stage to rotate the surgical platform for enhanced ergonomic comfort (for example, a right-handed operator may rotate the surgical platform counterclockwise for the drilling step).
Note: The gliding stage used is constructed of an upper aluminum plate that slides ±15 mm with respect to the fixed base plate.
- Gently grasp the superficial spinous process with forceps and lift the vertebra; the bone should lift away easily. If there is resistance, repeat bone thinning with the drill and if necessary use iris scissors, being careful to aim the scissor tips upward to avoid damaging the tissue.
Note: In order to maintain the dura intact, it is essential not to tug on the bone.
- Use #4 forceps to clear away any bone shards. Use a surgical spear to apply gentle steady pressure to control any bleeding. Rinse tissue with warm aCSF. Do not allow the tissue to dry out.

5. Cover-glass Implantation

- Gently apply a 3 mm borosilicate cover-glass to the exposed cord.
- Ensure agarose is cooled to 39 °C. Using a small spatula, apply warm 2% agarose/aCSF to the edge of the cover-glass and allow capillary action to draw it under the surface.
Note: At temperatures below 39 °C, the agarose may start to gel. If this occurs, rewarm using a water bath or microwave. Some operators prefer to first apply one drop of agarose and lay the cover-glass on top.
- Apply tissue adhesive to the exposed bony articular processes of the intact adjacent vertebra at thoracic level 11 vertebral spine and thoracic level 13 vertebral spine. Apply additional tissue adhesive in a ring around the laminectomy site, over the adjacent tendon and transverse process.
Note: Tissue adhesive is required for proper adherence of the dental cement in the subsequent steps. The articular processes form a natural seat on which the backplate can rest stably (**Figure 3**). Adhesion to the articular processes will form the strongest points of attachment.
- Mix dental cement with accelerant in a porcelain mixing tray. Utilize a small spatula to transfer dental cement onto the tissue adhesive layer. Use dental cement to adhere the backplate to the surgical field, centered over the window. Allow 10 minutes for the dental cement to cure.

Note: The firm adhesion of the backplate to the anterior and posterior articular processes provides the fundamental structural stability of the implant.

5. Use additional dental cement to fill in the interior base of the backplate, and the underside of the backplate : tissue interface.
Note: The extra application of dental cement improves adherence and reduces risk of leakage of microscope objective immersion fluid (saline) out the bottom of the backplate.
6. Advance the forked backplate holder to the appropriate position over the window. Secure the backplate into the backplate holder with screws.
Note: This protocol utilized a custom-machined backplate holder (**Figure 2G–H**).
7. Apply saline to the backplate to test for leakage. If any fluid leaks, dry the area and apply more dental cement.

6. Imaging Preparation

1. Transfer the animal on the surgical platform to the optical table.
Note: Our surgical platform, backplate holder, and isoflurane nose-cone holder can be transported between surgical and two-photon imaging stations as one unit, while applying continuous isoflurane anesthesia (**Figure 2D,H**). Similar units can be assembled from holding forks, beams, and supportive pillar posts obtainable from commercial sources (e.g. ThorLabs). For intravital microscopy, there should be at least 11 inches of clearance between the microscope objective and the optical table to accommodate the height of the surgical platform.
2. Affix the surgical platform to the optical table using a stainless-steel mounting post and counterbored clamping fork.
3. Apply fresh saline into the well of the backplate. Lower a water-immersion lens into the well.
4. Use transmitted or epifluorescence light to identify the area of interest and focus. Switch to laser scanning mode and perform *in vivo* imaging according to the appropriate two-photon laser excitation wavelength, dichroics and bandpass filters for the fluorophores present in the tissue⁶.

Representative Results

Implanted glass windows and intravital two-photon microscopy provides a useful tool for assessing dynamic changes in CNS proteins. The functional integrity of the BBB is influenced by the expression, subcellular localization, and turnover rates of tight junction proteins⁷. Previous studies have demonstrated that tight junction proteins undergo rapid and dynamic remodeling at steady state⁸. The currently described laminectomy and glass window preparation has been used in transgenic eGFP:Claudin-5 mice⁹, which bear fluorescent tight junction proteins, to assess BBB tight junction remodeling in the experimental autoimmune encephalomyelitis (EAE) model of multiple sclerosis¹⁰. In the representative data, imaging of eGFP:Claudin-5 was achieved with a two-photon microscope with 920 nm excitation, a 40× infrared objective (0.8 NA), and a green fluorescence emission filter (**Figure 4**). Optical stacks were sampled at 2 μm axial steps to 100 μm beneath the dural surface. Data depict visualization of the fluorescently labeled junctions throughout a vascular plexus. Single optical slices and Z-projection images are included (**Figure 4**). The clear delineation of tight junction structures in the Z-projection (**Figure 4B**) indicates that minimal X-Y image displacement is produced after successful laminectomy, window placement, and backplate implantation.

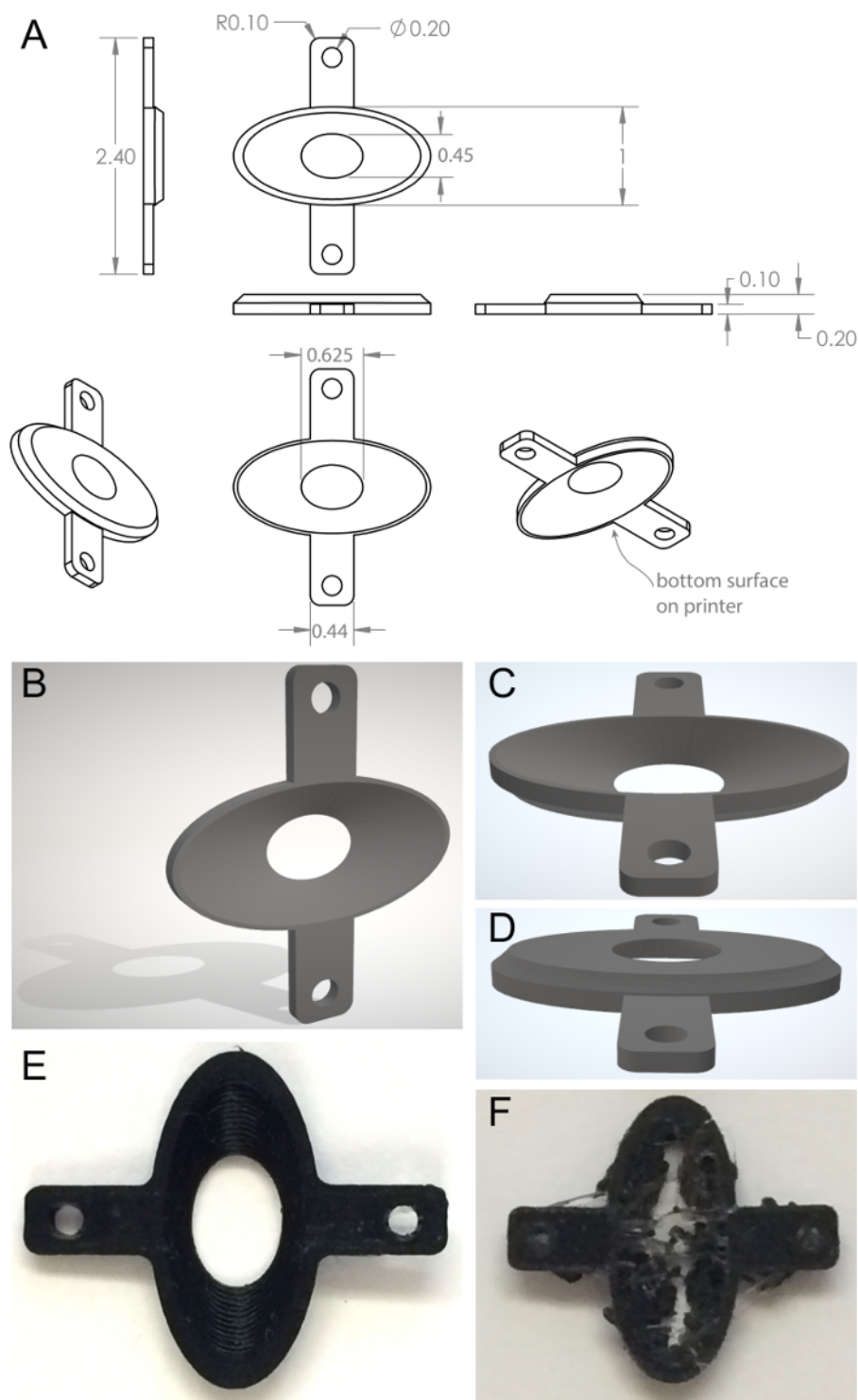


Figure 1. Custom printed backplate stabilization device. A) Orthogonal backplate views. B-D) Triangulated mesh models of dorsal and ventral surfaces of the backplate. E) Correctly printed backplate. F) Incorrectly printed backplate. See **Supplementary Files 1 and 2**. [Please click here to view a larger version of this figure.](#)

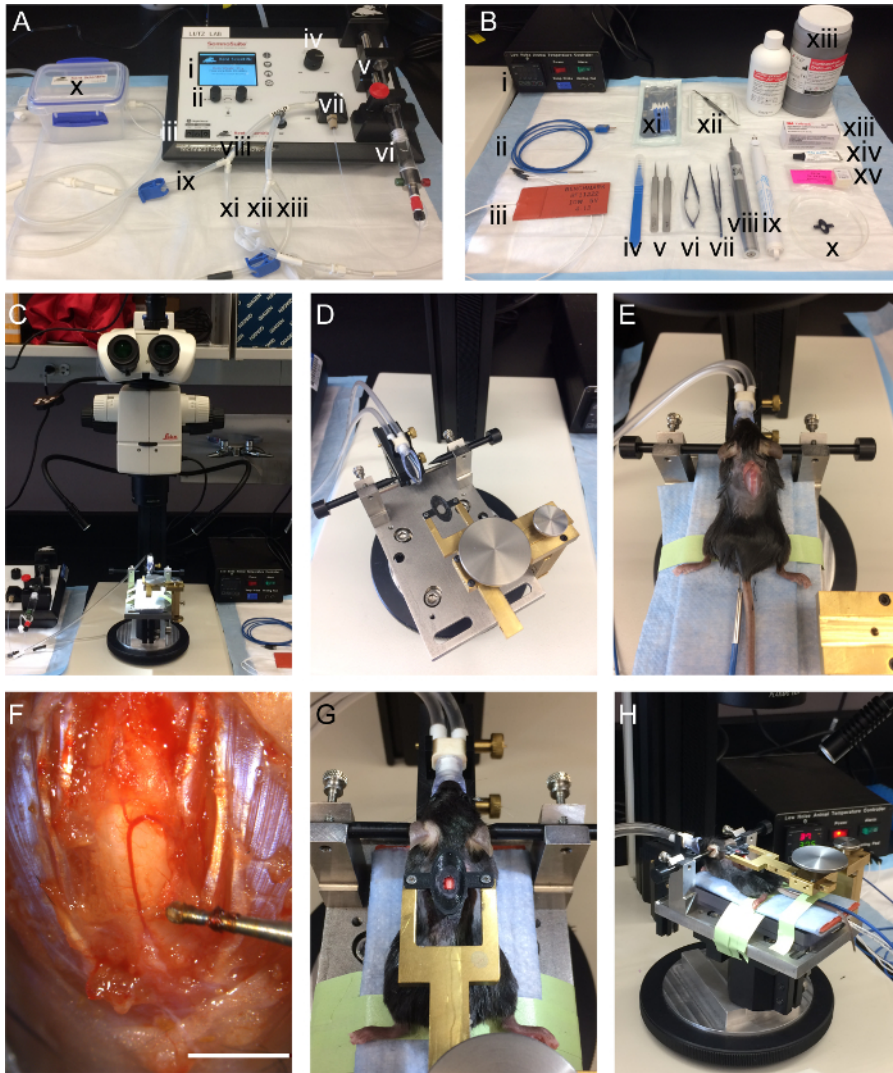


Figure 2. Surgical station for laminectomy. **A)** Isoflurane anesthesia delivery system utilizing an integrated digital vaporizer including (i) a touch screen display for controlling anesthesia, (ii) control dials, (iii) inputs for optional add-on physiology modules, (iv) anesthesia concentration adjustment knob, (v) syringe pump pusher block, (vi) syringe with isoflurane, (vii) integrated digital vaporizer, (viii) inspiration tubing, (ix) inspiration tubing for induction chamber, (x) induction chamber, (xi) inspiration tubing for nose-cone, (xii) expiration tubing for nose-cone, (xiii) expiration tubing for induction chamber. **B)** Instruments used in the laminectomy include (i) feedback controlled heating unit, (ii) K-coupled rectal thermometer probe, (iii) flexible silicone heating pad, (iv) #11 blade, (v) #5 forceps, (vi) toothed titanium forceps, (vii) titanium iris scissors, (viii) bone microdrill, (ix) cautery gun, (x) 3D printed backplate, (xi) absorbent foam surgical sponges, (xii) ceramic mixing tray for acrylic resin, (xiii) acrylic resin and accelerator, (xiv) tissue adhesive, (xv) ophthalmic lubricant, (xvi) 3 mm cover-glass. **C)** Stereomicroscope and surgical platform. During surgery, the surgical platform sits on a gliding stage (silver and black round base on microscope stage). **D)** Custom surgical platform. The isoflurane nose-cone holder is adjustable in the Y- and Z-axes to accommodate small and large mice. Ear bars stabilize the head with respect to the nose-cone. The brass fork is adjustable in X-, Y-, and Z-axes to for positioning over spinal cord laminectomy or cranial opening. The fork is mechanically anchored to the surgical platform to provide optimal stabilization of the imaging field during surgery and downstream applications including two-photon intravital microscopy. During surgery, the surgical platform is mounted on a gliding stage. **E)** Example of a mouse positioned with nose-cone, ear-bars, and rectal thermometer probe. **F)** Example of a surgical field after laminectomy. A bone drill is used to thin and remove residual vertebral bone. Scale bar is 2 mm. **G)** Oval backplate and glass window implanted onto the exposed spinal cord. **H)** Mouse positioned in the surgical station after completed laminectomy. [Please click here to view a larger version of this figure.](#)

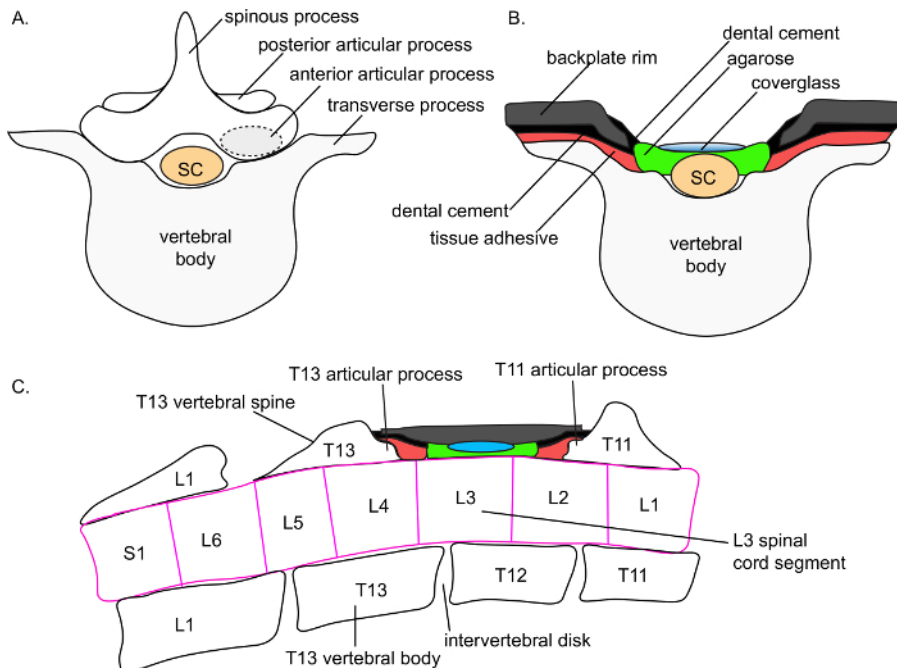


Figure 3. Schematic depiction of anatomic placement of the spinal cord window. **A)** Schematic depiction of the superior view of a lower thoracic vertebral body, spinous process, and spinal cord (sc) segment. A dotted circle depicts the seat of the articular process, the main support point for backplate adhesion. **B)** Schematic depiction of the superior view of the spinal cord window. The target vertebral spine (here, T12) has been removed. A thin layer of agarose overlays the spinal cord. A coverglass rests on top of the agarose. Tissue adhesive is applied over the transverse processes (and, not shown here, on the exposed articular process of the adjacent, intact vertebral spines). Dental cement overlays the tissue adhesive. The backplate adheres to the tissue cement, resting on the transverse processes (shown) and the articular process of the adjacent, intact vertebral spines (not shown in this panel). An additional thin layer of dental cement is applied on the interior of the backplate rim. The backplate is depicted in a cutaway view to visualize the cover-glass. **C)** Schematic depiction of the lateral view of the spinal cord window. The target vertebral spine (here, T12) has been removed. A thin layer of agarose overlays the spinal cord. A cover-glass rests on top of the agarose. Tissue adhesive is applied over the exposed articular process of the adjacent, intact T11 and T13 vertebral spines. Dental cement overlays the tissue adhesive. The backplate adheres to the tissue cement, resting on the transverse processes and the articular process of the adjacent, intact vertebral spines (shown). The backplate is depicted in a cutaway view; in a true lateral view the agarose and cover-glass would be obscured by the lateral wall of the backplate. Anatomic structures are based on detailed magnetic resonance imaging of the C57Bl/6 spinal column conducted by Harrison and colleagues¹¹. [Please click here to view a larger version of this figure.](#)

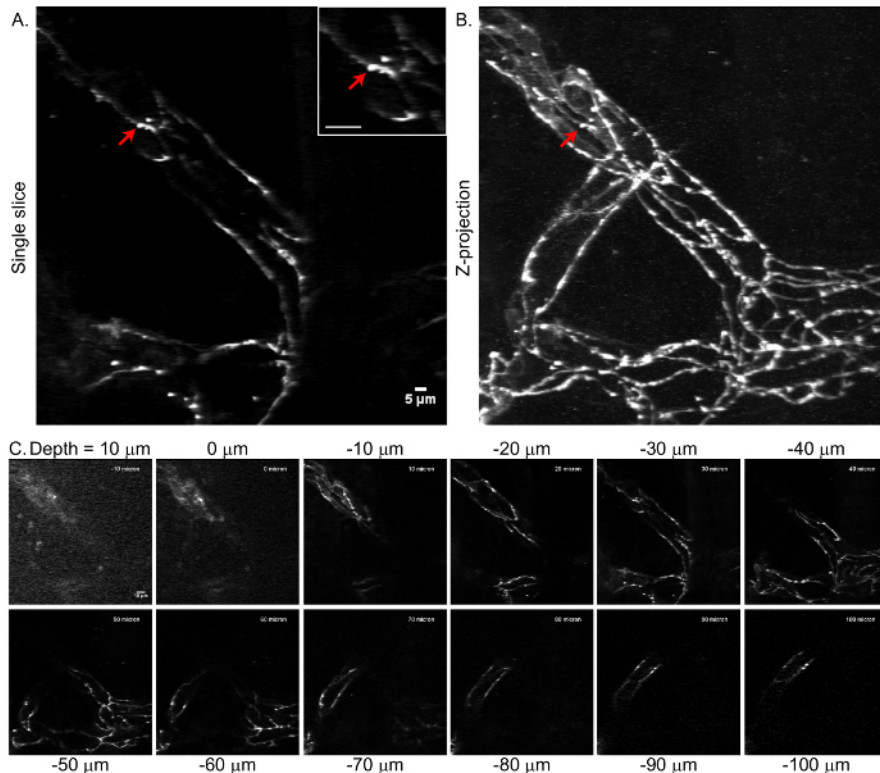


Figure 4. Tight junction microstructure visualized by eGFP:Claudin-5 in the mouse spinal cord by intravital two-photon microscopy.
A) Single optical section taken at 30 μm beneath the dural surface in a healthy eGFP:Claudin-5 mouse. Red arrow depicts an eGFP:Claudin-5 tight junction segment extending perpendicular to the longitudinal tight junction axis. Scale bar represents 5 μm . Inset: scale bar represents 10 μm . **B)** Z-projection of the vascular network extending 100 μm beneath the dural surface of the healthy mouse spinal cord. The optical stack was sampled at 2 μm axial step size and includes the slice from panel A. No image alignment has been performed. Sharp delineation of the junctional structures in the Z-projection demonstrates minimal image displacement between consecutive frames. **C)** Representative subset of optical slices taken at 10 μm intervals from the resultant Z-stack. [Please click here to view a larger version of this figure.](#)

Discussion

The method described here allows for stable imaging of the spinal cord in mice through a glass window. This method has been applied to assess BBB remodeling in transgenic eGFP:Claudin5 \pm mice that express a fluorescent BBB tight junction protein, but it could be applied equally well for studies of any fluorescent proteins or cells in the spinal cord.

Multiple methods for laminectomy and spinal cord stabilization have been developed. All protocols address stabilizing the spinal cord during imaging and window implementation for visual access to the structure of interest. The number of vertebra removed and the degree of invasiveness of the available protocols vary (e.g., components glued on the surface of superficial bone, as in the present protocol, *versus* embedded more deeply). Davalos and Akassoglou² developed a laminectomy method using removable clamps on each side of the spinal column and one clamp at the base of the tail of the mouse in order to stabilize the spinal cord. This innovative strategy to suspend the animal relieved some of the thoracic displacement caused by the movement of the lungs expanding against the surgical table. To create a well for containing immersion fluid for a water-immersion microscopic lens, a rim of gelatin seal (e.g. Gelseal) was made around the spinal cord and filled with aCSF. The seal rim could be disrupted during imaging, but could also be easily wiped away at the end of the session to enable wound closure and subsequent reimaging. This method has been widely adopted^{12,13}. Other groups have developed alternative stabilization methods. Fenrich *et al.*⁴ hand-prepared modified paper clips as a way to secure the spinal column. These modified paper clips were secured in the lateral vertebral pedicles with cyanoacrylate glue and maintained as permanently implanted handles for a removable external clip and external holding fork for excellent motion stability. Cupido and colleagues have presented variations on the aforementioned methods with incorporation of agarose overlaid onto the cord^{2,4,12}. Farrar and Schaffer³ developed a quadrilateral metal stabilizer that could allow for the implementation of a glass window onto three vertebrae rather than only one. This method also allowed the spinal cord to be attached with screws to a larger bridge stabilizer during imaging to reduce potential motion. A miniaturized one-photon microscope implanted directly onto the laminectomy imaging chamber has also been developed for *in vivo* recording in freely moving mice at the one-photon level, but is not yet readily available to most laboratories¹³. In a different approach, Weinger *et al.*¹ dissected an entire spinal cord and embedded it in agarose for *ex vivo* imaging, which allows for unsurpassable motion stability and access to the ventral spinal cord, but abrogates blood flow. Some limitations of these developments include lengthy surgical time⁴, possible disruption of the gelatin seal rim², the need to customize the cover-glass dimensions to fit the desired area of spinal cord⁴, manual modification of paper clips^{4,12}, relatively invasive surgical techniques^{12,14}, and air bubbles forming when using the silicon elastomer^{3,4}.

We have developed an alternative method that offers several advantages. This protocol has been optimized to reduce the amount of time spent during surgery. Whereas some surgical protocols require longer procedure times ranging from an hour and a half⁴ to an hour³; once mastered,

this laminectomy method can be performed in approximately 30 min. Reducing the time spent in surgery can decrease physiologic stress to the mouse, and facilitate higher-throughput experimentation. This protocol removes a single vertebra, and incorporates superficial adhesion of the stabilization device making it less invasive than some comparable protocols^{4,5,12,14}. Like the method of Figley *et al.*, by utilizing a plastic implant this protocol offers compatibility with acoustic imaging⁵.

To avoid light scattering (during intravital microscopy) that could be caused by the differences between the refractive indices of air, water, and tissue, most protocols overlay an optically transparent substrate over the exposed spinal cord. Common substrates include high purity, low-melting temperature agarose^{10,12} or silicone polymers^{3,4,5}. Agarose offers the advantage of ease of use, with minimal bubble formation, and is appropriate for acute imaging sessions. To protect the tissue from heat damage, it is convenient to heat the agarose to beyond the melting point and then allow it to cool to ~39 °C in a water bath during the laminectomy, so it can be ready at the appropriate time for application to the exposed spinal cord. For chronic imaging, silicone polymers are more resistant to dehydration. Pilot trials during the development of the current protocol omitted either the agarose layer or the overlying cover-glass, and found that the consequent light scatter reduced available depth of imaging.

A differentiating feature of this protocol is the incorporation of a 3D printed backplate and supportive backplate fork holder. After the laminectomy and window implantation, the preparation is stabilized by the addition of an 3D-printed oval backplate that is fixed in place with dental cement. The backplate serves two functions: first, it provides structural support and stabilization of the spinal cord, and second, it creates a lip to hold fluid for immersion objectives for microscopy. In prototypes of this setup, commercially available pillar posts, adaptors, and holding forks were used; we have recently switched to custom machined parts as depicted here. In either case, the essential feature is to provide structural rigor to stabilize the imaging field against the perturbations in space and time induced by heartbeat and respiration. Although the body of the animal is resting loosely on the heating pad, the spinal cord and its imaging field are slightly suspended from the holding fork, which also decreases respiratory displacement. The plastic substrate offers slight flexibility to accommodate tension from screwing into the plate holder. The black plastic color used for printing reflects minimal light into the fluorescence field. Through these methods, we successfully generate image stacks that can be used without *post hoc* alignment adjustment. Furthermore, the 3D backplate described herein is inexpensive to produce, costing only pennies in material for each print, once the printer is purchased. Furthermore, the costs of 3D printers have fallen in the recent years. The 3D printed backplate structural files (See **Supplementary Files 1 and 2**) published with this protocol can be readily modified to accommodate individual laboratory needs. We designed the long dimension of the backplate to accommodate the intervertebral space created by removal of thoracic 12 vertebral spine, which overlies the lumbar 2/3 spinal cord segments¹¹. To apply this technique to a different vertebral section, the accompanying CAD files can be modified.

This protocol utilizes a commercially available low-flow anesthesia system that deploys a digital integrated direct injection vaporizer as an alternative to the traditional passive vaporizer. The major feature of the low-flow unit is the reduced operator exposure to isoflurane, a substantial health benefit. The low-flow anesthesia unit also offers cost savings due to the reduced consumption of isoflurane and utilization of room air instead of compressed gas. In the present study, 2% isoflurane delivered by integrated digital vaporizer at 150 mL/min, together with feedback-controlled thermal support, achieved a stable plane of anesthesia and appropriate maintenance of core body temperature. Consistent with this, published comparisons of digital integrated vaporizers and traditional vaporizers have also concluded that the digital integrated vaporizer yields a stable plane of anesthesia and good preservation of core body temperature, heart rate, respiratory rate, and recovery while utilizing less isoflurane^{15,16}.

A non-steroidal anti-inflammatory drug (NSAID) such as carprofen can be administered Pre-operatively as a supplementary analgesic. Over the course of few hours, NSAIDs inhibit inflammatory cytokine transcription and interstitial edema; multi-day administration attenuates severity of neuroinflammatory diseases including experimental autoimmune encephalomyelitis, an animal model of multiple sclerosis^{17,18}. Particularly in the study of neuroinflammatory disease, the beneficial effects of carprofen analgesia must be carefully weighed against disease modifying effects when determining analgesia and anesthesia for an experiment in close coordination with appropriate regulatory boards.

A limitation of this method is that it is not readily amenable to repeated imaging sessions across multiple days. The main reason is that the backplate structure is too large to close the skin over. Therefore, there is a risk that a mouse would dislodge the backplate upon waking from anesthesia. If repeated imaging was essential, there are several strategies that could be deployed, including reducing the size of the backplate, or changing the mount. As with any surgical procedure, there is a learning curve for operators. Close coordination with institutional animal care offices and review boards is required.

Disclosures

The authors have nothing to disclose.

Acknowledgements

S.E. Lutz is supported by the National Center for Advancing Translational Sciences, National Institutes of Health, under Grant KL2TR002002 and University of Illinois Chicago College of Medicine start-up funds. Simon Alford is supported by RO1 MH084874. The content is solely the responsibility of the authors and does not necessarily represent the official views of the NIH. The authors thank Dritan Agalliu in the Department of Neurology at Columbia University Medical Center for the Tg eGFP:Claudin-5 mice, scientific discussions, and insights into the development of the surgical protocol and imaging applications. The authors thank Sunil P. Gandhi in the Department of Neurobiology and Behavior at University of California, Irvine for designing the first prototype of the stereotactic apparatus and animal temperature controller, discussion of the surgical protocol, and training in two-photon microscopy. The authors also thank Steve Pickens (W. Nuhsbaum, Inc.) for assistance in customizing the surgical stereomicroscope, and Ron Lipinski (Whale Manufacturing) for machining stereotactic parts.

References

1. Weinger, J. G. *et al.* Two-photon imaging of cellular dynamics in the mouse spinal cord. *Journal of Visualized Experiments*. (96), (2015).
2. Davalos, D., & Akassoglou, K. In vivo imaging of the mouse spinal cord using two-photon microscopy. *Journal of Visualized Experiments*. (59), e2760, (2012).
3. Farrar, M. J., & Schaffer, C. B. A procedure for implanting a spinal chamber for longitudinal *in vivo* imaging of the mouse spinal cord. *Journal of Visualized Experiments*. (94), (2014).
4. Fenrich, K. K., Weber, P., Rougon, G., & Debarbieux, F. Implanting glass spinal cord windows in adult mice with experimental autoimmune encephalomyelitis. *Journal of Visualized Experiments*. (82), e50826, (2013).
5. Figley, S. A. *et al.* A spinal cord window chamber model for *in vivo* longitudinal multimodal optical and acoustic imaging in a murine model. *PLOS ONE*. **8** (3), e58081, (2013).
6. Helmchen, F., & Denk, W. Deep tissue two-photon microscopy. *Nature Methods*. **2** (12), 932-940, (2005).
7. Liebner, S. *et al.* Functional morphology of the blood-brain barrier in health and disease. *Acta Neuropathologica*. **135** (3), 311-336, (2018).
8. Shen, L., Weber, C. R., & Turner, J. R. The tight junction protein complex undergoes rapid and continuous molecular remodeling at steady state. *Journal of Cell Biology*. **181** (4), 683-695, (2008).
9. Knowland, D. *et al.* Stepwise recruitment of transcellular and paracellular pathways underlies blood-brain barrier breakdown in stroke. *Neuron*. **82** 1-15., (2014).
10. Lutz, S. E. *et al.* Caveolin1 Is Required for Th1 Cell Infiltration, but Not Tight Junction Remodeling, at the Blood-Brain Barrier in Autoimmune Neuroinflammation. *Cell Reports*. **21** (8), 2104-2117, (2017).
11. Harrison, M. *et al.* Vertebral landmarks for the identification of spinal cord segments in the mouse. *Neuroimage*. **68** 22-29, (2013).
12. Cupido, A., Catalin, B., Steffens, H., & Kirchhoff, F. in *Laser Scanning Microscopy and Quantitative Image Analysis of Neuronal Tissue*. eds Lidia Bakota & Roland Brandt 37-50 Springer New York (2014).
13. Sekiguchi, K. J. *et al.* Imaging large-scale cellular activity in spinal cord of freely behaving mice. *Nature Communications*. **7** 11450, (2016).
14. Nadrigny, F., Le Meur, K., Schomburg, E. D., Safavi-Abbasi, S., & Dibaj, P. Two-photon laser-scanning microscopy for single and repetitive imaging of dorsal and lateral spinal white matter *in vivo*. *Physiological Research*. **66** (3), 531-537, (2017).
15. Adelsperger, A. R., Bigiarelli-Nogas, K. J., Toore, I., & Goergen, C. J. Use of a Low-flow Digital Anesthesia System for Mice and Rats. *Journal of Visualized Experiments*. (115), (2016).
16. Damen, F. W., Adelsperger, A. R., Wilson, K. E., & Goergen, C. J. Comparison of Traditional and Integrated Digital Anesthetic Vaporizers. *Journal of the American Association for Laboratory Animal Science*. **54** (6), 756-762, (2015).
17. Miyamoto, K. *et al.* Selective COX-2 inhibitor celecoxib prevents experimental autoimmune encephalomyelitis through COX-2-independent pathway. *Brain*. **129** (Pt 8), 1984-1992, (2006).
18. Muthian, G. *et al.* COX-2 inhibitors modulate IL-12 signaling through JAK-STAT pathway leading to Th1 response in experimental allergic encephalomyelitis. *Journal of Clinical Immunology*. **26** (1), 73-85, (2006).